

## TIME-LINEARISED CODE FOR SIMULATION OF UNSTEADY TRANSONIC FLOWS OVER AN AIRCRAFT WING WITH MOVING SHOCKS

Eddie Ly, John A. Gear and Hing Hung

Department of Mathematics  
 RMIT University, Melbourne, Victoria, AUSTRALIA

### ABSTRACT

We consider the unsteady flow as a small perturbation on the steady flow, which results in a pair of boundary value problems for the steady and first-order unsteady reduced potentials. The resultant equations are solved numerically using the type-dependent finite difference schemes incorporating the method of false transients and line relaxation. The effects of the shock motion are investigated and the amplitudes of the shock motion are explicitly estimated based on the time-linearised solutions.

### INTRODUCTION

An obvious reason for studying unsteady flows is the prediction of the effect of unsteady aerodynamic forces on a flight vehicle, since these effects tend to increase the likelihood of aeroelastic instabilities. This is a major concern in the aerodynamic design of aircraft that operate in the transonic regime, where the flows are characterised by the presence of adjacent regions of subsonic and supersonic flow, usually accompanied by weak shocks. The location, strength and amplitude of the shocks are dependent on time.

Due to the ease of practical implementation in aeroelastic applications, time linearisation is attractive for flutter computations. That is we consider the unsteady flow as a small perturbation on the steady flow, which results in a pair of boundary value problems for the steady and first-order unsteady reduced potentials. The governing equation for the two-dimensional steady flow is the nonlinear Transonic Small Disturbance (TSD) Equation. The first-order unsteady equation is linear, and for the harmonic boundary disturbances considered, its reduced wave equation form is of mixed elliptic/hyperbolic type, depending upon the nature of the steady solution. Both steady and unsteady equations are solved by type-dependent finite difference schemes, and the shock amplitudes are explicitly estimated.

Time-linearised results, generated by the schemes, for transonic flow past a NACA 64A006 aerofoil with an

oscillating flap are presented. Comparisons with the result obtained from a time marching finite difference scheme (developed by the authors, see Gear, Ly and Phillips (1997)) and the experimental data of Tijdeman and Schippers (1974) are made.

### MATHEMATICAL FORMULATIONS

A nearly planar wing is immersed in an unsteady, isentropic and inviscid flow, and assumed to have an infinite aspect ratio, so that the flow field around the aerofoil is the same for any cross section perpendicular to the wing. The unsteady TSD Equation for the reduced potential,  $\phi(x, z, t)$ , may be written as

$$M^2 \frac{\partial}{\partial t} (\phi_t + 2\phi_x) + \frac{\beta^2}{2\bar{u}} \frac{\partial}{\partial x} (\bar{u} - \phi_x)^2 - \frac{\partial}{\partial z} \phi_z = 0, \quad (1)$$

where the constants are given by

$$\beta^2 = 1 - M^2, \quad \bar{u} = \frac{\beta^2}{M^2(\gamma + 1)}.$$

Equation (1) is locally of hyperbolic type representing supersonic flow for  $\phi_x > \bar{u}$  and of elliptic type representing subsonic flow for  $\phi_x < \bar{u}$ , and its solution contains discontinuous jumps that represent shocks. Here  $(x, z)$  represents a nondimensional rectangular Cartesian coordinate system with the aerofoil chord length as the characteristic lengthscale,  $t$  is the nondimensional time variable,  $\gamma$  is the ratio of specific heats and  $M$  is the freestream Mach number. In nondimensional terms the fluid velocity is given by  $\mathbf{v} = \nabla(x + \phi)$ .

On the wing the flow must be tangent to the surfaces at all points, thus the following physical boundary condition is imposed along  $x \in [0, 1]$ ,

$$\phi_z(x, 0^\pm, t) = h_x^\pm(x, t) + h_t(x, t). \quad (2)$$

The upper and lower wing surfaces are defined by  $z = h^\pm(x, t)$ , respectively. Behind the wing, the Kutta condition requires that at the trailing edge and across the wake there be no jump in normal velocity

or pressure, and hence for isentropic flow no jump in density. Far away from the wing, nonreflecting far-field boundary conditions are employed, see Gear, Ly and Phillips (1997) and Ly, Gear and Phillips (1997).

Any shock that exists in the flow field must satisfy the shock jump relation derived from the conservation form of Equation (1), namely

$$M^2 \langle \phi_t + 2\phi_x \rangle \langle \phi_x \rangle \frac{d\Lambda}{dt} + \frac{\beta^2}{\bar{u}} (\bar{u} - \overline{\phi_x}) \langle \phi_x \rangle^2 + \langle \phi_z \rangle^2 = 0, \quad (3)$$

together with the condition derived from the assumption of irrotationality,

$$\theta_{sw} = \left. \frac{dx}{dz} \right|_{sw} = -\frac{\langle \phi_z \rangle}{\langle \phi_x \rangle}. \quad (4)$$

Here  $\overline{\phi_x}$  is the average value of  $\phi_x$  across the shock,  $\langle \phi_x \rangle$  is the jump in  $\phi_x$  across the shock (downstream minus upstream) and  $\Lambda(t)$  is the instantaneous shock position; the subscript sw denotes the quantity evaluated at the shock surface. The shock speed and angle (relative to the positive  $z$ -axis) are measured by  $d\Lambda/dt$  and  $\theta_{sw}$ , respectively.

The unsteady motion of an aircraft can be assumed to consist of a steady component plus a small harmonically oscillating unsteady component. That is,

$$h^\pm(x, t) = h_s^\pm(x) + h_o(x) e^{ikt}, \quad (5)$$

$$\phi(x, z, t) = \phi_s(x, z) + \phi_o(x, z) e^{ikt}, \quad (6)$$

where the subscripts s and o denote the steady and oscillatory components,  $i = \sqrt{-1}$  and  $k$  is the reduced frequency or Strouhal number (a parameter that measures the unsteadiness of the flow). Assumptions (5) and (6) have the advantage of suppressing the time dimension of the computation, but they restrict the study to linear harmonic motions and result in two coupled governing equations.

To facilitate the use of high density grid meshing along the aerofoil surfaces and in regions containing the shock, without using a vast number of grid points, shearing transformations are employed. In general terms the transformation is given by

$$\xi = \xi(x), \quad \zeta = \zeta(z), \quad (7)$$

where  $\xi$  and  $\zeta$  are the nondimensional computational coordinates in the  $x$  and  $z$  directions, respectively.

We find that by substituting assumptions (5) and (6) into (1) and (2), and separating steady and oscillatory components in the nondimensional computational domain,  $\phi_s(\xi, \zeta)$  satisfies

$$\frac{\beta^2}{2\bar{u}} \xi_x \frac{\partial}{\partial \xi} (\bar{u} - \xi_x \phi_{s\xi})^2 - \zeta_z \frac{\partial}{\partial \zeta} (\zeta_z \phi_{s\zeta}) = 0, \quad (8)$$

with wing boundary condition, for  $\xi \in [0, 1]$ ,

$$\zeta_z(0) \phi_{s\zeta}(\xi, 0^\pm) = \xi_x h_{s\xi}^\pm(\xi). \quad (9)$$

The oscillatory component,  $\phi_o(\xi, \zeta)$ , satisfies

$$\left[ 2iM^2k - \frac{\beta^2}{\bar{u}} \xi_x \frac{\partial}{\partial \xi} (\bar{u} - \xi_x \phi_{s\xi}) \right] \xi_x \phi_{o\xi} - \zeta_z \frac{\partial}{\partial \zeta} (\zeta_z \phi_{o\zeta}) - M^2k^2 \phi_o = 0, \quad (10)$$

with wing boundary condition, for  $\xi \in [0, 1]$ ,

$$\zeta_z(0) \phi_{o\zeta}(\xi, 0^\pm) = \xi_x h_{o\xi}(\xi) + ikh_o(\xi). \quad (11)$$

It is noted that Equation (10) is linear, but of the same mixed elliptic/hyperbolic type as (8). In general  $\phi_o$  is complex, thereby permitting phase shifts between the field quantities and the boundary disturbance.

## NUMERICAL PROCEDURES

The solution for  $\phi_s$ , which does not depend on  $\phi_o$ , is obtained by the method of false transients, as described in Ly, Gear and Phillips (1997, 1998). The solution is then used in the solution process for the corresponding  $\phi_o$ . This approach has the benefit that  $\phi_s$  need not be regenerated for each unsteady boundary disturbance or reduced frequency of interest.

Second-order accurate central difference formulae are employed for the  $\zeta$  - derivative terms and the term  $\phi_{o\xi}$  in (10). The  $\xi$  - derivative terms are approximated using the second-order Engquist-Osher operators (Engquist and Osher, 1980). As the flow changes from subsonic to supersonic the type-dependent difference operators smoothly change from central difference approximations (to account for the domain of dependence of elliptic region) to upwind difference approximations (to account for the absence of downstream influence in hyperbolic region). This ensures a smooth transition from subsonic to supersonic flow. Hence entropy violating decompression shocks will not develop. As the flow changes from supersonic to subsonic the type-dependent operator changes to an appropriate shock point operator (Murman and Cole, 1971). Note that the type-dependent operators have been modified by the authors, see Gear, Ly and Phillips (1997), to produce sharper shock profiles with little overshoot behind the shock.

## Line Relaxation Technique

Approximating Equation (10) by the appropriate difference operators and applying the boundary conditions results in a system of simultaneous equations for the value of  $\phi_o$  at each grid point. The solution is found by a successive line relaxation along a vertical line of grid points at constant  $i$  for each iteration

number,  $n$ . The equation system can be written as

$$[C]_i \{\tilde{\phi}_o\}_i^{n+1} = \{g\}_i, \quad (12)$$

where  $\{\tilde{\phi}_o\}_i$  and  $\{g\}_i$  are column vectors of length km, and  $\{\tilde{\phi}_o\}_i = [\tilde{\phi}_{o,i,1}, \tilde{\phi}_{o,i,2}, \dots, \tilde{\phi}_{o,i,km}]^T$ . The km  $\times$  km dimensional tridiagonal matrix,  $[C]_i$ , is a function of  $\phi_s$  only, while  $\{g\}_i$  is a function of  $\phi_s$ ,  $\phi_{o,i-3,k}^{n+1}$ ,  $\phi_{o,i-2,k}^{n+1}$ ,  $\phi_{o,i-1,k}^{n+1}$  and  $\phi_{o,i+1,k}^n$ . Convergence rate can be enhanced by including the following relaxation process,

$$\{\phi_o\}_i^{n+1} = \omega \{\tilde{\phi}_o\}_i^{n+1} + (1 - \omega) \{\phi_o\}_i^n, \quad (13)$$

where  $\{\tilde{\phi}_o\}_i^{n+1}$  is the solution to (12). Initially  $\phi_o$  is zero everywhere except on the wing where  $h_o$  is nonzero. The scheme successively sweeps from upstream to downstream boundary during which new values of  $\phi_o$  are obtained from (12) and updated using (13), iteratively.

The stability and convergence rate of the line relaxation technique depend on the choice of relaxation parameters  $\omega$  in (13). The values of  $\omega$  depend on the type of flow, and from the numerical experimentations, the acceptable values have been found to be  $\omega \approx 1.5$  in subsonic region, and  $\omega \approx 0.85$  in supersonic region where the scheme is required to be under relaxed rather than over relaxed, so that convergence difficulties are less likely to occur due to the presence of supersonic points in the flow field. This phenomenon was also observed by Murman and Cole (1971).

### NORMAL SHOCK RELATIONS

In this section we investigate a method of determining the amplitude of the shock motion explicitly based on the time-linearised solution. In two-dimensional small perturbation transonic flows the shocks that usually occur are nearly normal to the flow direction. Thus we can assume that if the steady flow has a shock, then this shock may be approximated by a normal shock relation in our schemes.

We expressed the instantaneous shock position,  $\Lambda$ , as

$$\Lambda(t) = \Lambda_s + \Lambda_o e^{ikt}. \quad (14)$$

Linearising the reduced potential (Fung, Yu and Seebass, 1978) about  $x = \Lambda_s$  and using the assumptions (6) and (14), we obtain to the first-order approximation

$$\phi(\Lambda, \zeta, t) \approx \phi_s(\Lambda_s, \zeta) + [\phi_o(\Lambda_s, \zeta) + \Lambda_o \xi_x(\Lambda_s) \phi_{s\xi}(\Lambda_s, \zeta)] e^{ikt}. \quad (15)$$

On the shock surface we require  $\langle \phi \rangle = 0$ , hence

$$\langle \phi_s(\Lambda_s, \zeta) \rangle = 0, \quad (16)$$

$$\langle \phi_o(\Lambda_s, \zeta) \rangle = -\Lambda_o \langle \xi_x(\Lambda_s) \phi_{s\xi}(\Lambda_s, \zeta) \rangle, \quad (17)$$

and the latter relation is used to estimate  $\Lambda_o$  at the wing surfaces.

### NUMERICAL RESULTS

The pressure distributions computed for a NACA 64A006 aerofoil with a quarter-chord flap oscillating at a frequency of 120 Hz, reduced frequency of 0.235, freestream Mach number of 0.875, and at amplitudes ( $\Delta\delta$ ) of  $1.5^\circ$  and  $1^\circ$  are collected in Figures 1 and 2, respectively. Since we are dealing with zero incidence and mean flap angle, the steady flow is symmetric. The shock amplitudes and the unsteady pressures on the upper and lower aerofoil surfaces are equal in magnitude, but differ by  $180^\circ$  in phase angle. Therefore only the pressure coefficient,  $C_p$ ,

$$C_p(x, z, t) = -2(\phi_x + \phi_t), \quad (18)$$

$$= C_{ps}(x, z) + C_{po}(x, z) e^{ikt}, \quad (19)$$

on the upper surface are presented, and  $C_p/C_p^* > 1$  indicates locally supersonic flow, where  $C_p^*$  is the critical pressure coefficient,  $C_p^* = -2\bar{u}$ .

The time-linearised results correspond reasonably well with the experimental data of Tijdeman and Schippers (1974), as illustrated in Figure 1. The jump in  $C_{ps}$  locates the steady shock position,  $\Lambda_s$ , and the second pressure peak of  $|C_{po}/\Delta\delta|$  locates the flap hinge. The unsteady aerodynamic quantities, such as the normal force coefficient,  $k_c$ , and moment coefficient about quarter chord,  $m_c$ , are computed by integration of the oscillatory pressure distributions, and the comparisons with those obtained from the experiment are presented in Table 1. It is important to note that the experimental technique used to measure unsteady pressures was sensitive only to the first harmonic, so that the present results and experimental data are being compared on the same basis.

In Figure 2 the time-linearised results are compared to those from the time marching scheme for a complete period of flap oscillation. The pressure distributions before and after the shocks are in good agreement, except for the shock positions since the shock oscillations are not implicitly incorporated into the scheme. We also observe that the shock in the steady field requires a corresponding shock in the unsteady perturbation field, which in effect results in harmonic changes in shock strength. The shock was estimated (using (14) with (17)) to oscillate over a distance of 2% of the chord length, while the time marching scheme predicted 6%.

| Results      | Re $k_c$ | Im $k_c$ | Re $m_c$ | Im $m_c$ |
|--------------|----------|----------|----------|----------|
| Experimental | 0.629    | -0.558   | 0.805    | -0.375   |
| Numerical    | 0.787    | -0.550   | 0.922    | -0.314   |

Table 1: Comparisons of aerodynamic coefficients.

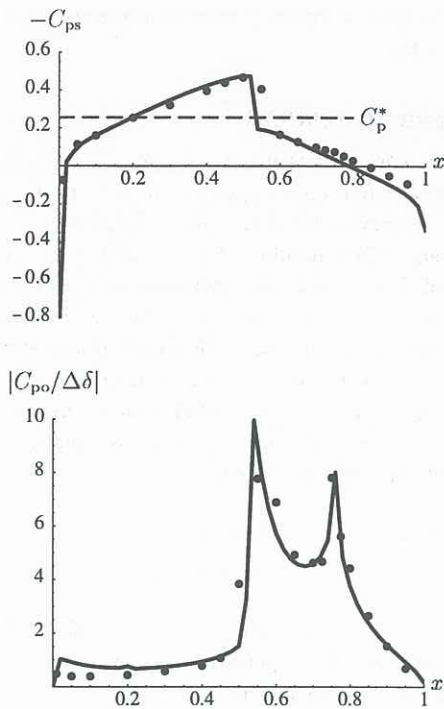


**Figure 1:** Comparisons of the numerical (solid lines) and experimental (dots) results.

## CONCLUSIONS

A treatment of unsteady transonic flow as a small perturbation about the nonlinear small disturbance steady flow has been applied to a NACA 64A006 aerofoil with an oscillating flap. It has been found that for the line relaxation scheme to be stable, the relaxation parameter must be less than one when the scheme sweeps across supersonic regions. The comparisons of the present result to the experimental data show good qualitative agreement, except for some quantitative discrepancies which would seem to be related mainly to viscous effects (not accounted for in the present formulation), and to possible wind tunnel wall or three-dimensional flow effects in the experimental data. From the numerical experimentations, it is evident that shock strengths, locations, and amplitudes must be accurately represented if unsteady transonic pressures and loads are to be predicted satisfactorily. In future work we hope to include implicitly the shock oscillations into our line relaxation scheme by updating the oscillatory solution for the grid points just behind the shock via the oscillatory component of the shock jump condition. We will also investigate the relationship between the shock amplitudes and the reduced frequencies.

## REFERENCES

ENGQUIST, B. and OSHER, S., "Stable and entropy satisfying approximations for transonic flow calculations", *Maths. Comput.* **34**, 149, Jan. 1980, 45-75.

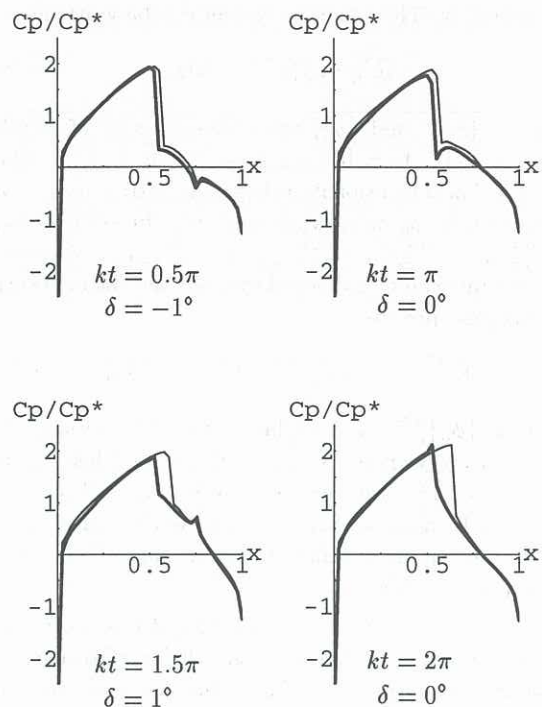


**Figure 2:** Comparisons of the time-linearised (thick lines) and time marching (thin lines) results where  $\delta$  is the flap angle. The flap is down/up when  $\delta$  is positive/negative.

FUNG, K.Y., YU, N.J. and SEEBASS, R., "Small unsteady perturbations in transonic flows", *AIAA J.* **16**, 8, Aug. 1978, 815-822.

GEAR, J.A., LY, E. and PHILLIPS, N.J.T., "Time marching finite difference solution of the modified Transonic Small Disturbance Equation", in *Proc. of the Comput. Tech. & Appl.: CTAC97*, B.J. Noye, M.D. Teubner and A.W. Gill, ed., World Scientific, 1997, pp. 209-216.

LY, E., GEAR, J.A. and PHILLIPS, N.J.T., "Improved approximate factorisation algorithm", in *Proc. of the Comput. Tech. & Appl.: CTAC97*, B.J. Noye, M.D. Teubner and A.W. Gill, ed., World Scientific, 1997, pp. 393-400.

LY, E., GEAR, J.A. and PHILLIPS, N.J.T., "Simulated shock motion using a time-linearised transonic code", in *Proc. of the 3rd Biennial Eng. Maths. & Appl. Conf.: EMAC '98*, E.O. Tuck and J.A.K. Stott, ed., The IEAust and The Eng. Maths. Group, Australia, 1998, pp. 331-334.

MURMAN, E.M. and COLE, J.D., "Calculation of plane steady transonic flows", *AIAA J.* **9**, 1, Jan. 1971, 114-121.

TIJDEMAN, H. and SCHIPPERS, P., "Results of pressure measurements on a lifting airfoil with oscillating flap in two-dimensional high subsonic and transonic flow", Tech. Rep. NLR TR 73018 L, National Aerospace Lab. NLR, The Netherlands, Nov. 1974.